

Preparation of single-walled carbon nanotube reinforced magnesia films

Chunsheng Du and Ning Pan¹

Nanomaterials in the Environment, Agriculture, and Technology (NEAT),
University of California, Davis, CA 95616, USA

E-mail: npan@ucdavis.edu

Received 9 July 2003, in final form 6 October 2003

Published 26 November 2003

Online at stacks.iop.org/Nano/15/227 (DOI: 10.1088/0957-4484/15/1/041)

Abstract

Single-walled carbon nanotube (SWNT)/MgO composite films were fabricated by growing carbon nanotubes while simultaneously sintering a MgO film. The effect of iron and molybdenum concentrations in liquid catalysts and the effect of the density of carbon nanotubes in the composite films on the quality of the films were investigated. Microstructure analysis showed that SWNTs were uniformly grown in the MgO film. The presence of a controlled amount of carbon nanotubes in MgO films is believed to greatly improve the performance of the composite films as well as impart new functions. These MgO/nanotube composite films are expected to have a very high second-electron emission, which is very desirable for use in vacuum electronic devices.

1. Introduction

Magnesia layers has been increasingly noted for their advantages as a key element of plasma display panels (PDPs) [1–5]. It protects the dielectric layer above the electrodes from sputtering while yielding a high ion-induced secondary electron emission (SEE) coefficient. The SEE generated by the primary electrons in a magnesia film can move to the surface with relatively weak electron–electron scatterings due to the absence of free electrons in insulators [2]. Due to its large SEE yield and good resistance to sputtering, the MgO layer plays an essential role in keeping the operating voltage relatively low and also limiting the damages due to energetic ions. MgO layers are important both for efficacy and lifetime issues [1].

The combination of the emissive and protective properties of MgO layers make them unique. These layers have been used in the PDP industry since their introduction in the 1970s by Uchiike *et al* [6], in spite of many attempts to find materials with better properties. For example, Bachmann *et al* [7] showed that carbon nanotubes by vapour deposition (CVD) diamond coating can have SEE yield value as large as MgO for neon ions and much larger than MgO for xenon ions. Yi *et al* [3] obtained very large SEE values of maximum 15 000 when a MgO film was deposited on randomly oriented multi-walled carbon nanotubes (MWNTs), which is much higher

than the SEE yield from a single crystal MgO (25 at the best) and porous MgO (about 1000 under high electric field). The high SEE yield of MgO coated MWNTs in their study was believed to result from the high electric field achieved at the tip of carbon nanotubes due to their high aspect ratios and small tip radii of curvature. More recently, Kim *et al* [2], Heo *et al* [4] and Lee *et al* [5] acquired unusually high SEE yield of greater than 22 000 (beyond the limit of the detector) by depositing MgO thin films on vertically grown MWNTs.

However, MgO coated carbon nanotubes still resemble the morphology and macrostructure of nanotubes in those studies, and therefore their protective properties are not more advantageous than those of MgO films for practical applications even though their SEE yield is very high. It can be conceived that a MgO thin film with appropriate amount of carbon nanotubes dispersed in it should have a combination of very high SEE yield and good protective property. In addition, since single-walled carbon nanotubes (SWNTs) have a much smaller diameter than multi-walled ones, much higher SEE yields may be expected for SWNTs if high aspect ratio and small tip radii of curvature are the key elements to achieve high electric fields at the tip of nanotubes. So it may be beneficial to prepare SWNT reinforced MgO thin film for potential application in PDPs.

Here, we report a very simple method to fabricate such films. This method has the advantages of growing SWNTs in a MgO matrix while simultaneously sintering MgO film in

¹ Author to whom any correspondence should be addressed.

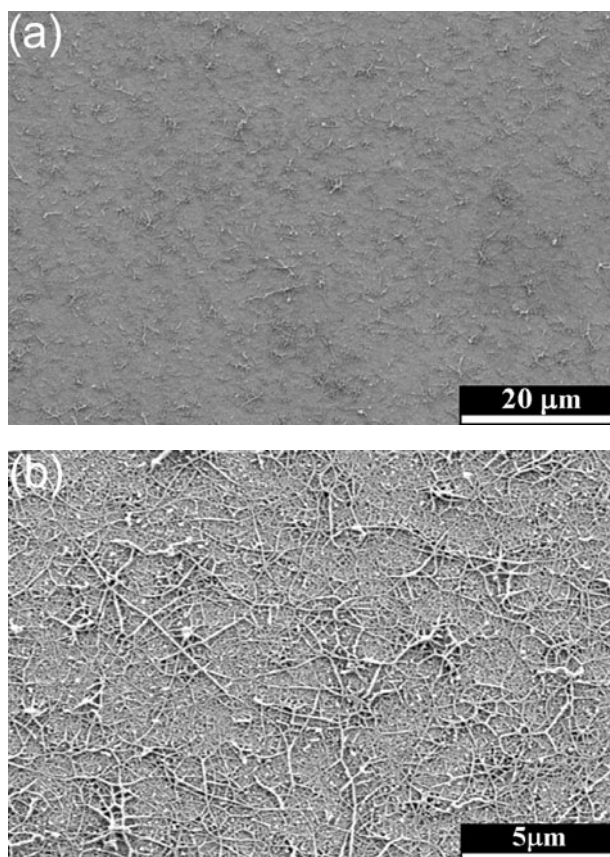


Figure 1. SEM images of surface structure of sample A. (a) General view of the film. (b) Carbon nanotubes embedded in MgO film.

one simple step. Moreover, the SWNTs can effectively prevent cracking of the MgO film during preparation and also increase the flexibility of the film due to the remarkable mechanical properties [8, 9], which are always desired in the fabrication of thin films.

2. Experimental details

In our experiments, quartz sheets were used as the substrate for MgO films, and were cleaned by sonicating in acetone for 10 min. Magnesium precursor solution, which also acts as liquid catalyst in our experiments, was prepared in the way widely used for preparation of liquid catalyst in studies for surface growth of carbon nanotubes [10–15]. Briefly, a solution was prepared using 0.31 mmol of ferric nitrate nonahydrate (EM Science) and 0.053 mmol of molybdenyl acetylacetonate (Acros) dissolved in 10 ml of methanol, and then this solution was added to a solution of magnesium nitrate hexahydrate (Fisher Scientific) in 10 ml of ethanol together with 0.5 g of block copolymer (BASF Corporation). Several solutions with different molar ratios of Fe:Mo:Mg were prepared.

The quartz substrates were dipped into the liquid catalysts for 5 s and then dried at room temperature before annealed at 500 °C for 0.5 h to eliminate the copolymer before loading into a tube furnace to simultaneously carry out both chemical growth of CVD and sintering of MgO film as well. Hydrogen was introduced into the furnace while the furnace was heated

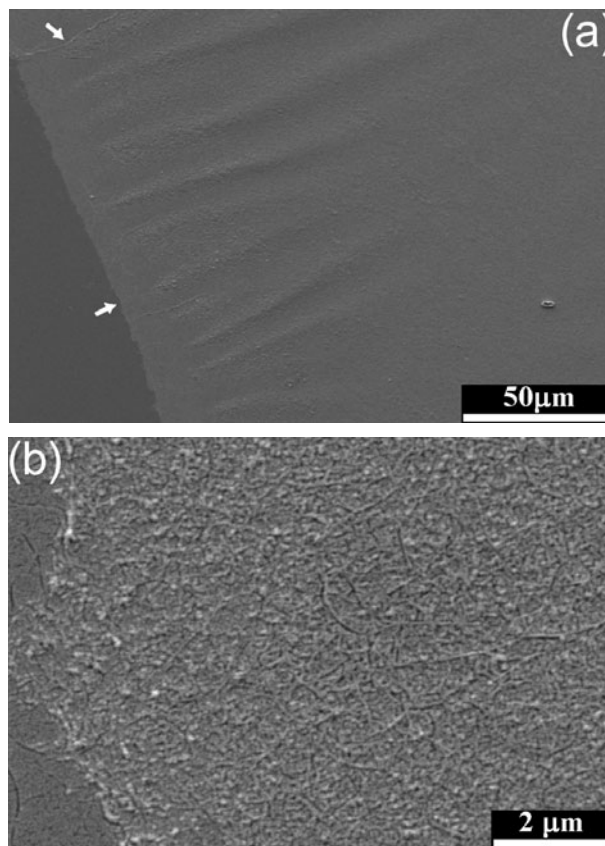


Figure 2. SEM images of surface structure of sample A after acid treatment. (a) Low magnification image showing the pleats in the sample. (b) High magnification image showing detail of the structure of the surface.

up to 950 °C and held for 15 min during which methane was introduced. Methane supply was then shut off and the system was cooled to room temperature.

Three samples were prepared using liquid catalysts with different molar ratios of Fe:Mo:Mg, and were denoted for convenience as sample A (with high iron concentration); sample B (with medium iron concentration) and sample C (with very low iron concentration). Samples were characterized by scanning electron microscopy (SEM) (Philips XL30), transmission electron microscopy (TEM) (model: Philips CM 120) and x-ray diffraction (XRD). Elemental analysis was carried out on FEI XL30-SFEG high-resolution SEM equipped with energy dispersive x-ray spectroscopy (EDS) system.

3. Results and discussion

Figure 1 shows the surface microstructure of sample A after the CVD growth of carbon nanotubes. The film is relatively smooth and no cracks are visible. At higher magnification, some carbon nanotubes are exposed on the surface of the MgO film; the majority of these tubes are embedded in the film with only parts of the tubes shown on the surface. Because the incubation period of carbon nanotubes is only about less than 10 s and the growth rate of nanotubes ranges from several nanometres to 100 nm s⁻¹ [16, 17], the carbon nanotubes can be initiated and grow much longer right in the MgO matrix before the film is fully sintered. For those tubes grown close

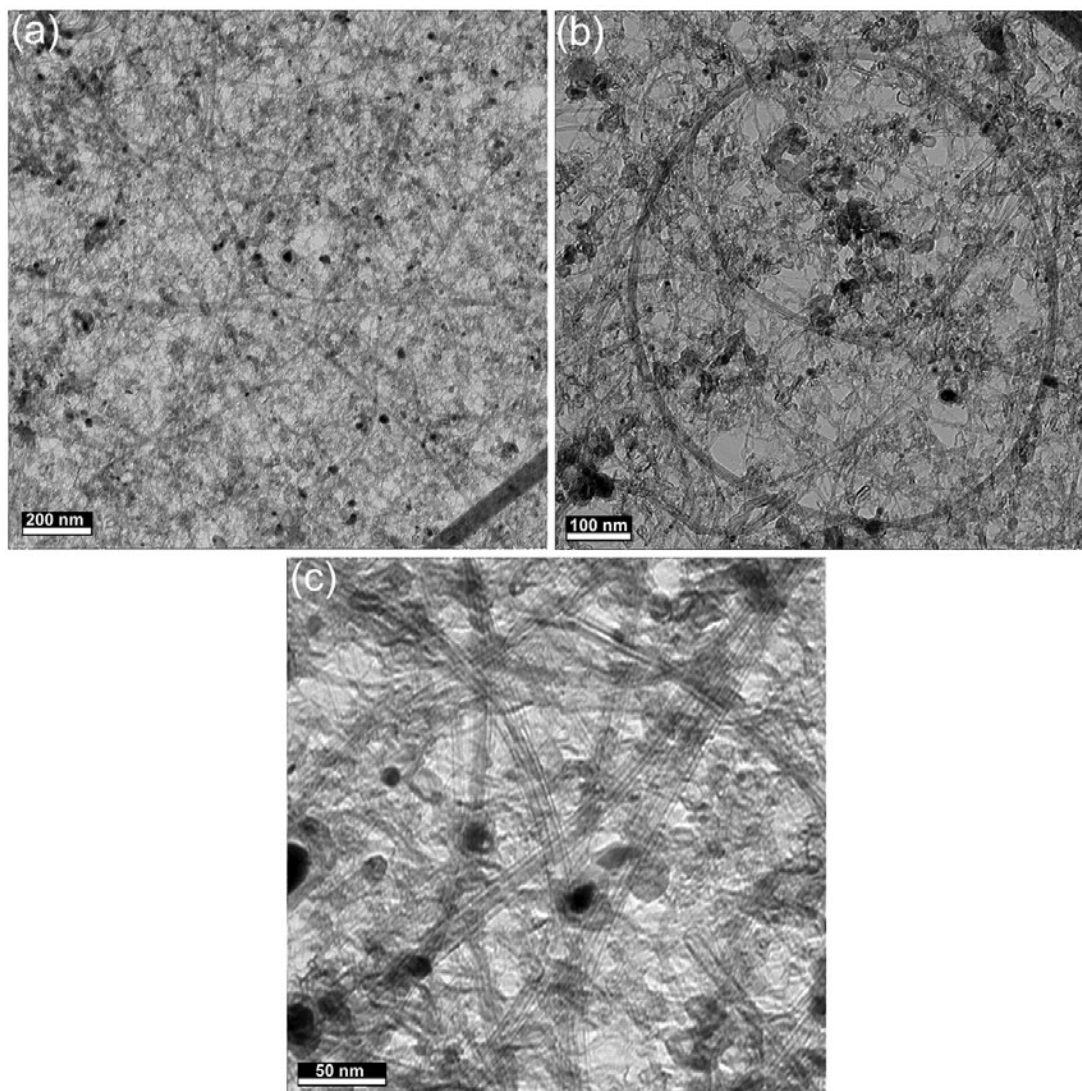


Figure 3. TEM images of sample A. (a) Low magnification image showing the dispersion and density of nanotubes in the film. (b) Typical bundles forming ring observed in the film. (c) High resolution image showing that the nanotubes are SWNTs.

to the film surface, part of them may protrude from the MgO film surface.

The produced film can be easily separated from the quartz substrate by simply immersing the whole system into aqueous hydrochloride acid overnight. We speculate that the MgO film did not form a very dense crystalline structure that is largely acid resistant, for it was sintered for only 15 min. Thus this technique allows the transfer of the whole MgO film onto other substrates of given interest.

Figure 2 shows the SEM images of the film transferred onto a glass plate (the arrow in the SEM image shows the boundary of the film). It should be noticed that some pleats were formed in the area adjacent to boundary of the layer, indicating that the layer is likely to be very flexible. A higher magnification SEM image (figure 2(b)), in comparison with figure 1(b), shows that there are fewer tubes anchored on the surface of the film after acid treatment, possibly due to the removal of a thin layer of the MgO film. Thus, most of the tubes detected in figure 2(b) are actually in the matrix

before acid treatment, and this was further confirmed by TEM analysis. Since the film is very thin and almost transparent, we can then transfer a small portion onto a copper grid to conduct a TEM analysis of the microstructure and dispersion of carbon nanotubes in the MgO matrix. Recall that a very thin layer has already been eliminated from the MgO film after the acid treatment, so any carbon nanotubes detected under TEM should not be the tubes on the surface of MgO film shown in figure 1(b). Figure 3 shows typical TEM images of the transferred piece. From figure 3(a), we can see that there are many carbon nanotubes in bundle form, whereas there are very few carbon nanotubes shown on the surface of the acid-treated MgO film as shown in figure 2(b). Note that the analysed area corresponding to figure 3(a) is much smaller than that in figure 2(b), however the tube density shown in figure 3(a) is much higher than that detected under SEM in figure 2(b). So we believe that most of the carbon nanotubes detected under TEM are inside the MgO matrix instead of at the surface, and thus this film can be called MgO/NTs composite film. Since the film is very thin, it is very difficult to measure its exact

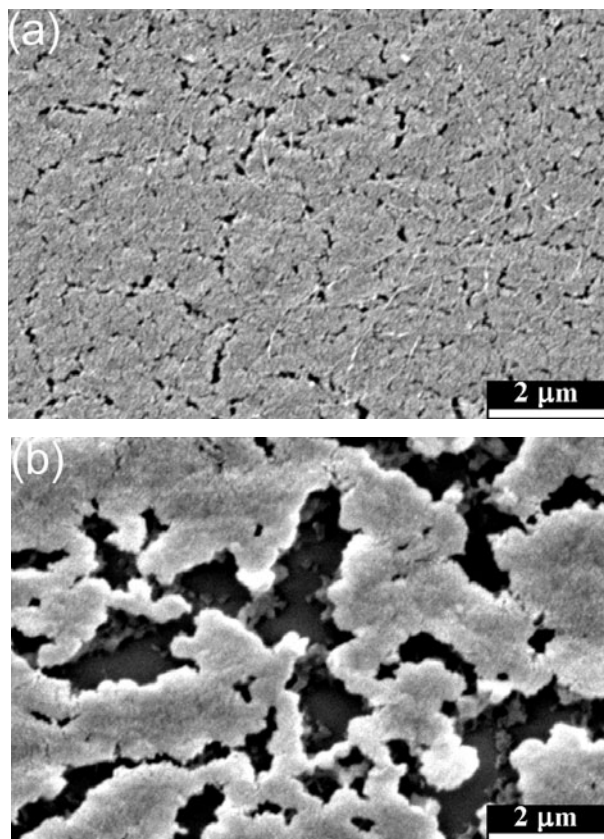


Figure 4. SEM images of surface structure of samples prepared from liquid catalysts with lower iron concentration: (a) sample B, (b) sample C.

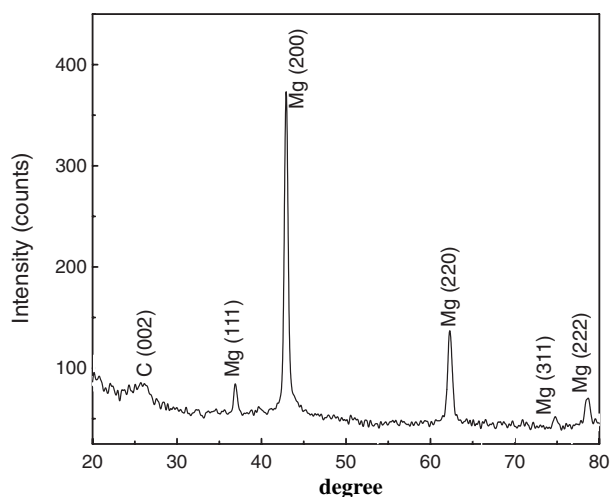


Figure 5. XRD pattern of sample A.

thickness, which we estimated it to be around several tens of nanometres from the SEM images shown in figure 2.

It should also be noted that there are some black particles in the film shown in the TEM images in figure 3. These are iron particles too big to initiate growth of carbon nanotubes under the conditions of this experiment. There are also some carbon nanotube bundles which formed rings in the sample, and this is also observed by other researchers of these MgO systems [18].

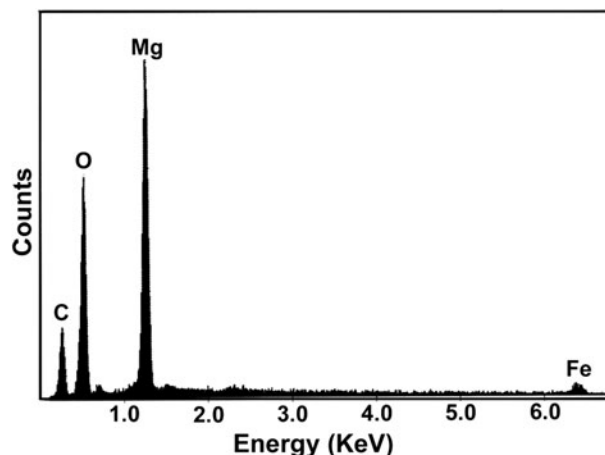


Figure 6. EDS pattern of sample A.

High resolution TEM imaging (figure 3(c)) shows that the nanotubes are single-walled with a diameter around 2–3 nm. According to Yi *et al* [3], the high SEE yield of MgO-coated MWNTs leads to the strong electric field emission achieved at the apexes of nanotubes, because of their small tip radii of curvature. It is reasonable to expect that an even stronger field emission can be achieved using our MgO film where SWNTs are present in the matrix, since their diameter is much smaller than that of MWNTs.

In addition, we also found that the existence of SWNTs in MgO reinforces the film and prevents cracking. As mentioned earlier, pleats were formed in the film during the transfer without causing any cracking, indicating that this composite film was highly flexible, which we attribute to the presence of the SWNTs. This was further confirmed by numerous cracks observed (figure 4) in samples B and C (the composite films prepared from liquid catalyst with lower iron concentrations). The low iron concentration during CVD growth means that few carbon nanotubes can be initiated during CVD growth. As illustrated in figure 4, there are far fewer tubes on the surface of the films in sample B, and almost no tubes in sample C; this should also be true for the overall tube density in the film. Correspondingly, there are many cracks in these two samples. It can be deduced from microscopy observations that the presence of appropriate amounts of SWNTs in MgO films is very helpful to obtain high quality MgO composite films. The SWNTs have two functions. Firstly, they can effectively reinforce the film because of their unique mechanical properties [8, 9]. Secondly, SWNTs can deform to a certain degree [19–22] to release the stress built up in the MgO film and thus prevent the film from cracking.

Sample A was further characterized using XRD and EDS analyses. Figure 5 shows the XRD pattern of sample A. It can be seen that the diffraction peaks assigned to MgO periclase dominate the XRD pattern, causing the (002) graphite peak assigned to carbon nanotubes to be less intense, which was also observed by other researchers [23]. Figure 6 shows the EDS pattern of sample A, indicating that a small amount of iron particles remains in the composite film because the carbon layer outside of the particles prevented them from reacting with acid during the acid treatment. EDS quantitative analysis showed that the atomic ratio of carbon to magnesium is 5.04.

In summary, a very simple method to fabricate thin MgO/SWNT composite films has been presented. Controlling the iron concentration in the liquid catalyst can manipulate the density of SWNTs grown in the MgO film. This method produces flexible and crack-free composite films which can easily be transferred to any other desired substrates. The existence of SWNTs in the MgO thin film enhances the integrity of the MgO film and provides a superior potential electric field enhancer. This composite film will be useful for applications in various vacuum electronic devices.

Acknowledgments

Financial support from Mytitek Corporation (Davis, California) is gratefully acknowledged. The authors would also like to thank the BASF Corporation (Mount Olive, New Jersey) for supplying the block copolymer, and David Heldebrandt for helpful suggestions.

References

- [1] Boeuf J P 2003 *J. Phys. D: Appl. Phys.* **36** R53–79
- [2] Kim W S, Yi W, Yu S, Heo J, Jeong T, Lee J, Lee C S, Kim J M, Jeong H J, Shin Y M and Lee Y H 2002 *Appl. Phys. Lett.* **81** 1098–100
- [3] Yi W, Yu S G, Lee W, Han I T, Jeong T, Woo Y, Lee J, Jin S, Choi W, Heo J, Jeon D and Kim J M 2001 *J. Appl. Phys.* **89** 4091–5
- [4] Heo J N, Kim W S, Jeong T W, Yu S G, Lee J H, Lee C S, Yi W K, Lee Y H, Yoo J B and Kim J M 2002 *Physica B* **323** 174–6
- [5] Lee J, Jeong T, Yua S G, Jin S, Heo J, Yi W, Jeon D and Kim J M 2001 *Appl. Surf. Sci.* **174** 62–9
- [6] Uchiike H, Miura K, Nakayama N, Shinoda T and Fukushima Y 1976 *IEEE Trans. Electron Devices* **23** 1211–7
- [7] Bachmann P K, van Elsbergen V, Wiechert D U, Zhong G and Robertson J 2001 *Diam. Relat. Mater.* **10** 809–17
- [8] Treacy M M J, Ebbesen T W and Gibson J M 1996 *Nature* **381** 678–80
- [9] Li F, Cheng H M, Bai S, Su G and Dresselhaus M S 2000 *Appl. Phys. Lett.* **77** 3161–3
- [10] Franklin N R and Dai H J 2000 *Adv. Mater.* **12** 890–4
- [11] Kong J, Soh H T, Cassell A M, Quate C F and Dai H J 1998 *Nature* **395** 878–81
- [12] Gu G, Philipp G, Wu X C, Burghard M, Bittner A M and Roth S 2001 *Adv. Funct. Mater.* **11** 295–8
- [13] Li Q W, Hao Y, Li X H, Zhang J and Liu Z F 2002 *Chem. Mater.* **14** 4262–6
- [14] Li Q W, Yan H, Cheng Y, Zhang J and Liu Z F 2002 *J. Mater. Chem.* **12** 1179–83
- [15] Yan H, Li Q W, Zhang J and Liu Z F 2002 *Carbon* **40** 2693–8
- [16] Bower C, Zhou O, Zhu W, Werder D J and Jin S H 2000 *Appl. Phys. Lett.* **77** 2767–9
- [17] Bower C, Zhu W, Jin S H and Zhou O 2000 *Appl. Phys. Lett.* **77** 830–2
- [18] Colomer J F, Henrard L, Flahaut E, Van Tendeloo G, Lucas A A and Lambin P 2003 *Nano Lett.* **3** 685–9
- [19] Chopra N G, Benedict L X, Crespi V H, Cohen M L, Louie S G and Zettl A 1995 *Nature* **377** 135–8
- [20] Hertel T, Walkup R E and Avouris P 1998 *Phys. Rev. B* **58** 13870–3
- [21] Ruoff R S, Tersoff J, Lorents D C, Subramoney S and Chan B 1993 *Nature* **364** 514–6
- [22] Yu M F, Lourie O, Dyer M J, Moloni K, Kelly T F and Ruoff R S 2000 *Science* **287** 637–40
- [23] Rana R K, Koltypin Y and Gedanken A 2001 *Chem. Phys. Lett.* **344** 256–62